Chemosphere 162 (2016) 117–124

Contents lists available at ScienceDirect

Chemosphere

journal homepage: www.elsevier.com/locate/chemosphere

Influence of silver nanoparticles on heavy metals of pore water in contaminated river sediments

Wei Tao [a, b], Guiqiu Chen [a, b, *], Guangming Zeng [a, b, **], Ming Yan [a, b], Anwei Chen [c], Zhi Guo [a, b], Zhenzhen Huang [a, b], Kai He [a, b], Liang Hu [a, b], Lichao Wang [a, b]

[a] College of Environmental Science and Engineering, Hunan University, Changsha 410082, PR China
[b] Key Laboratory of Environmental Biology and Pollution Control (Hunan University), Ministry of Education, Changsha 410082, PR China
[c] College of Resources and Environment, Hunan Agricultural University, Changsha 410128, PR China

HIGHLIGHTS

- AgNPs caused heavy metals to be transferred from surface water to sediment.
- Heavy metals were released to water phase in ionic form after sedimentation.
- Hg^{2+} was reduced to Hg^0 and formed Ag-Hg amalgam in sediment pore water.

GRAPHICAL ABSTRACT

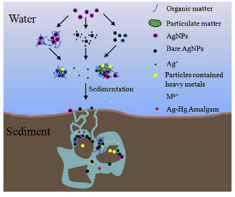

ARTICLE INFO

Article history:
Received 4 March 2016
Received in revised form
11 July 2016
Accepted 14 July 2016

Handling Editor: Tamara S. Galloway

Keywords:
Silver nanoparticles
Xiangjiang river
Pore water
Heavy metal
Amalgam

ABSTRACT

Despite the increasing knowledge on the discharge of silver nanoparticles (AgNPs) into the environment and their potential toxicity to microorganisms, the interaction of AgNPs with heavy metals remains poorly understood. This study focused on the effect of AgNPs on heavy metal concentration and form in sediment contaminated with heavy metals from the Xiangjiang River. The results showed that the concentration of Cu, Zn, Pb and Cd decreased and then increased with a change in form. The changes in form and concentrations of heavy metals in pore water suggested that Cu and Zn were more likely to be affected compared to Pb and Cd. The concentrations of Hg in sediment pore water in three AgNPs-dosed containers, increased greatly until they reached their peaks at 4.468 ± 0.133, 4.589 ± 0.235, and 5.083 ± 0.084 μg L^{-1} in Bare AgNPs, Citrate AgNPs and Tween 80 AgNPs, respectively. The measurements of Hg concentrations in the sediment pore water, combined with SEM and EDX analysis, demonstrated that added AgNPs stabilized in pore water and formed an amalgam with Hg^0, which can affect Hg transportation over long distance.

1. Introduction

With a significant increase in development of nanotechnology, greater attention is being paid to the pollution by engineered nanomaterials (ENMs). The latter is a new class of pollutants, and, little information is currently available on their potential environmental impacts. ENMs have unique properties that emerge at small dimensions. It has been shown that the same properties may also have adverse effects on organisms once they were released to the environment (Shoults-Wilson et al., 2013) while the magnitude of these adverse effects depends on the characteristics, concentration, bio-availability, and transformations of ENMs in the environment.

In recent years, there has been a great focus on testing the toxicity of Ag nanoparticles (AgNPs), because AgNPs are one of the

* Corresponding author. College of Environmental Science and Engineering, Hunan University, Changsha 410082, PR China.
** Corresponding author. College of Environmental Science and Engineering, Hunan University, Changsha 410082, PR China.
E-mail addresses: gqchen@hnu.edu.cn (G. Chen), zgming@hnu.edu.cn (G. Zeng).

http://dx.doi.org/10.1016/j.chemosphere.2016.07.043
0045-6535/

most commonly used ENMs in consumer products, serving mainly as antimicrobial agents. The widespread use of AgNPs can result in leaching of AgNPs into natural water from manufacturing and disposal of consumer products without entering wastewater treatment (Benn and Westerhoff, 2008; Jones and Hoek, 2010; Mueller and Nowack, 2008), even though municipal wastewater treatment plants have a high removal efficiency of AgNPs (Li et al., 2013).

River sediment is a main potential place ENMs would end up through spillage, discharge, atmospheric deposition, soil runoff, or STP discharge waters (Blaser et al., 2008; Boxall et al., 2007; Mueller and Nowack, 2008). The wider production and use of ENMs will inevitably result in their release into the river system. The Xiangjiang River is one of the tributaries of the Yangtze River in China, and the largest river in Hunan province, has a surface area of 94,600 km^2, and a total length of 856 km. Many large cities, such as Changsha, Xiangtan and Zhuzhou, are located in the middle and lower reaches of the Xiangjiang River. The mining and metallurgical industries are highly developed in this basin. The Xiangtan Steel Group, Zhuzhou Metallurgical Corporation and Shuikoushan Mining Bureau are distributed along the lower reaches of the river (Mao et al., 2014). The Xiangjiang River has suffered from substantial metal contaminations because of urbanization and industrialization. In some areas, the concentration of Cd, Zn, and Cu transcended the standard values of Grade III standard of China environmental quality standard for soil (GB15618-1995) by 10–170 times, 2.2–10.2 times and 1.4 times, respectively (Zhu et al., 2012).

Numerous studies have demonstrated that AgNPs can be toxic to bacteria (Jeon et al., 2003; Bosetti et al., 2002), invertebrates (Bielmyer et al., 2002), algae and plants (Lee et al., 2012; He et al., 2012), or it can stimulate the activity of microorganisms (Guo et al., 2016; Zuo et al., 2015). However, the extent of toxicity of AgNPs varies with water chemistry and sediment characteristics (Chambers et al., 2014) possibly because AgNPs interact with natural aquatic colloids after their release. This can affect the stability and subsequent environmental behavior of both AgNPs and aquatic colloids (Lin et al., 2010). Trace metals can be associated with particles and colloids, which play an important role in heavy metal transport, and can be affected by AgNPs (Vignati and Dominik, 2003).

To assess the potential risk of ENMs entering the river system, we need to understand the role that water chemistry and sediment characteristics play on ENMs stability, mobility and toxicity. The transformation and toxicity of ENMs have been widely studied in both laboratory and field experiments (Unrine et al., 2012a, 2012b; Lowry et al., 2012). While these studies have provided a valuable insight into the mechanisms that control the transformation and toxicity of ENMs, the influence of ENMs on heavy metals in natural river systems were ignored, even in systems that are severely contaminated with heavy metals.

To better understand the influence of AgNPs on river sediments that have been contaminated with heavy metals, AgNPs with three different kinds of coatings were synthesized in the laboratory and characterized by ultraviolet–visible (UV–vis) spectrophotometry, dynamic light scattering (DLS). Hollow fiber membranes were used to collect sediment pore water, without disturbing the sediment environment. In order to analyze the change of heavy metal concentration and morphology induced by AgNPs in contaminated sediments, the total and colloidal concentrations of different heavy metals in pore water at different times were determined. These data together with the results from scanning electron microscopy (SEM) and energy-dispersive X-ray (EDX) analysis facilitated clarification of the mechanisms involved in the concentration and morphology change of heavy metals in sediment pore water.

2. Materials and methods

2.1. Synthesis and characterization of AgNPs

Three types of AgNPs were prepared in this study. The preparation followed the method of previous studies (Kvitek et al., 2008), with some minor modifications. 4 mL of 10 mM $AgNO_3$ and 20 mL of 20 mM $NH_4 \cdot OH$ were mixed in a 100 mL beaker and were vigorously stirred with a magnetic stir bar. Then 2 mL of 0.1 M NaOH was added to adjust the pH value of the solution to 12 and 16 mL of 25 mM D-maltose was added into the mixture to form silver nanoparticles. Citrate AgNPs and Tween 80 AgNPs were prepared by adding pre-calculated volumes of the bare silver nanoparticle stock suspension and either trisodium citrate or Tween 80 into a 50 mL polycarbonate centrifuge tube in order to achieve 1 mM trisodium citrate or 10 mM Tween 80. NaCl, Na_2CO_3 and NaOH were added to adjust the ionic strength to 1 mM and pH at 7.0 ± 0.3, respectively. The tubes were sealed and shaken for 24 h in the dark at room temperature (22 °C). Dialysis was conducted using cellulose ester membranes (Spectra/Pro® Biotech) with a molecular weight cut off of 8–10 kDa for Bare AgNPs and Citrate AgNPs and 50 kDa for Tween 80 AgNPs. The Ag concentrations of AgNPs stock solutions were measured by flame atomic absorption spectrometry (AAS700, PerkinElmer, USA), after HNO_3 digestion. The dissolved fraction of the AgNPs stock solution was less than 1%, as determined by analyzing the filtrate of ultrafiltration centrifuged stock suspension (Amicon Ultra-0.5 3 K centrifugal tube, Millipore), using ICP-OES (IRIS Intrepid II XSP, Thermo Electron Corporation, USA). The UV absorption spectrum of the stock AgNPs suspensions was measured using a UV–visible light spectrophotometer at wavelength between 300 and 600 nm (Model UV-2550, Shimadzu, Japan). AgNPs size distributions were determined using a Zetasizer Nanoseries (Malvern Instruments) with a 633 nm laser source and a detection angle of 173°.

2.2. Sediment source and characterization

Laboratory experiments were performed with sediments contaminated with heavy metals and surface water from the Xiangjiang River. Sediments and surface water were collected from the Xiangjiang River under the forth bridge on the river as shown in Fig. 1. Sediments were processed with a 2 mm sieve, in order to remove large debris. Porosity was determined by drying 5 cm^3 sediment samples at 80 °C for 48 h. Total organic carbon (TOC) was measured with a TOC analyzer (TOC-VCPH, Shimadzu, Japan), after acidifying 0.1 g of dried sediment with 2 mL of 4 M HCl (non-oxidizing acid which has little influence on organic materials), in order to remove inorganic carbon (Rawlins et al., 2008; Edmondson et al., 2015). TOC of sediment was measured for soil background check, the deviation won't affect our experiment. Total bulk sediment metal concentrations were measured by inductively coupled plasma atomic emission spectrometry (ICP-AES, PS-6, BAIRD) after microwave-assisted acid digestion following USEPA method 3051 A. Sediment characteristics and element concentrations are shown in Table S1.

2.3. Experimental setup

The experiments were performed in plastic containers with two rows of holes in the wall equipped with pore water collection equipment. The pore water collection equipment consisted of a PVDF hollow fiber membrane (pore size 1 μm) with both ends in a plastic hose of 3 mm diameter, forming a closed circle, and a plastic needle stuck through the container wall into the other end of the plastic hose. All joints were sealed with 707 silicone rubbers. All

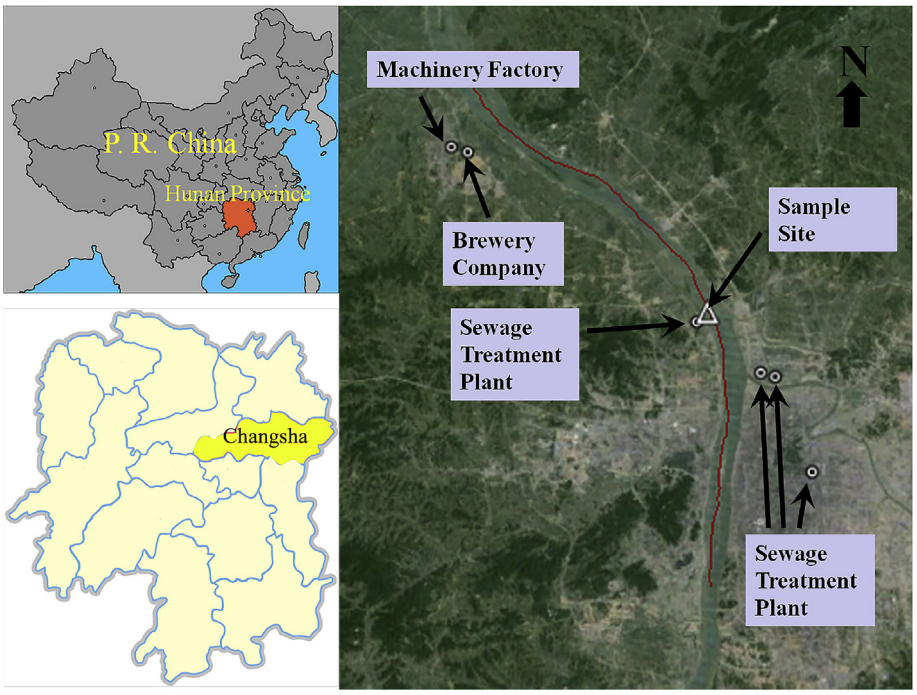

Fig. 1. Location of the sampling site and the pollutant sources near the sampling site.

parts of the device are non-metallic. (See Supporting Information for details).

Sieved sediments were gently added into the containers, without bending the pore water drawing equipment, in order to form a 10 cm sediment bed with a flat surface following the pumping of 2 L of surface water into each of the containers. This was done drip-by-drip, using a peristaltic pump (Cole-Parmer, Masterflex C/L) to minimize the disturbance of the sediment-water interface (SWI). The two rows of holes for pore water collection equipment were 1 and 3 cm below the SWI, respectively. Then the containers were left to stabilize for 3 months in dark-light condition and constant temperature.

2.4. Experimental procedure

At day 0, $AgNO_3$ prepared in ultra-pure water with $AgNO_3$ salt (Sigma-Aldrich, UK) and three types of fresh synthesized AgNPs, were added to four containers, respectively in order to achieve a nominal target concentration of 100 μg L^{-1}, while a control container received no AgNPs or $AgNO_3$. Aliquot samples were taken at specific time intervals (0, 1, 3, 5, 8, 11, 15, 20, 30, 50 and 70 days) for analysis.

Sediment pore water was directly withdrawn into a polycarbonate centrifuge tube using a peristaltic pump. In a small aliquot, pH was measured immediately after sampling with an FE20 laboratory pH meter (FE20 Mettler Toledo, Shanghai, China). TOC was determined with a TOC analyzer. The SO_4^{2-} and Cl^- concentrations were determined using an ion chromatograph (ICS-900, DIONX, USA). Then the solution was divided into two parts, one part was filtered through a 3 kDa cellulose nitrate membrane filter (Millipore, MA, USA) using a peristaltic pump, while the other part was not filtered. Both were acidified to 5% HCl and stored in plastic tubes at 4 °C until analysis. For Hg analysis, both were acidified to 5% HCl, BrCl were added to oxidize Hg to Hg^{2+}, and stored in glass vials at 4 °C until analyzed by cold vapour Atomic Fluorescence Spectrophotometer (AFS-9700, Haiguang, Beijing, China). All analysis was completed within 24 h. The amount of colloids was calculated by the differences between the unfiltered concentration and the filtered concentration. All of the data were obtained from triplicate assays, and then analyzed with Origin 8.0 software or mapped with Sigmaplot 10.0.

2.5. SEM and EDX analysis

For TEM analysis, colloids in 5 mL unfiltered pore water were centrifuged onto 400 mesh Cu grids. The grids were rinsed in O_2-free ultra-pure water, dried, and stored until analysis. Colloid morphology and composition were studied by SEM and EDX analysis. Colloids were investigated in a SEM (FEI Quanta 200), which was operated at an accelerating voltage of 30 kV. The microscope was operated in scanning mode. Colloids were localized and analyzed for their elemental composition, using an EDX analysis system (EDAX Inc, Mahwah, NJ, USA).

3. Results and discussion

3.1. Characterization of synthesized AgNPs

AgNPs were successfully synthesized, as indicated by the color change of the solution, which turned yellow. Characteristics of the three pristine AgNPs are described in Fig. S2. The absorption peak of the synthesized Bare AgNPs was 397 nm, and because of the coating, the absorption peak of Citrate AgNPs and Tween 80 AgNPs were 400 nm and 405 nm, respectively. DLS results showed that the mean hydrodynamic diameters of synthesized AgNPs in ultrapure water were approximately 26.10 ± 0.94, 27.46 ± 0.91 and 30.12 ± 0.76 nm, respectively (Fig. S2 B, C, and D). The Ag concentration of Bare AgNPs, Citrate AgNPs and Tween 80 AgNPs after dialysis were 28.6, 12.8, and 13.2 mg L^{-1}, respectively.

3.2. Dissolution, aggregation and sedimentation in surface water

During the experiment, pH of the containers of overlying water dropped from 7.52, 7.54, 7.57, 7.59, and 7.55 to 7.45, 7.36, 7.47, 7.32, and 7.45 in Bare AgNPs, Citrate AgNPs, Tween 80 AgNPs, $AgNO_3$, and control container, respectively, as shown in Fig. S3A. The addition of AgNPs and $AgNO_3$ did not significantly affect the pH of the water column which remained near neutral with a slight decreasing tendency which was probably caused by the dissolution of CO_2. The TOC of all four dosed containers in the overlying water dropped dramatically, while the control one experienced very little change at day 1 (Fig. S3B). After day 1, the TOC of all four dosed containers in the overlying water started to increase and reached an equilibrium, apart from the Tween 80 AgNPs dosed one, which decreased after reaching a peak of 6.14 mg L^{-1} at day 5. AgNPs and $AgNO_3$ rapidly settled out from the water column in the first 5 days, which was indicated by the rapid drop of total Ag concentration below the detection limit (2 μg L^{-1}) (Fig. S4). This might have been due to the relatively high concentration of Ag relative to the water content, and AgNPs would react strongly with organic matter and deposite causing TOC concentration to drop according to previous research (Piccapietra et al., 2012). In the first 2 h, Ag concentration decreased faster in citrate AgNPs container than in Tween 80 AgNPs container, which is different from Li's research that the sterically dispersed Tween 80 AgNPs released Ag^+ faster than did bare AgNPs and citrate AgNPs (Li and Lenhart, 2012). This might be the reason that bare AgNPs and citrate AgNPs aggregated and deposited faster than Tween 80 AgNPs, causing more Ag loss in the water column. The Tween 80 AgNPs-dosed container resulted in more Ag in the water column within 120 h, but a similar decreasing rate in total Ag in the water column was observed for the four dosing containers. This indicates that the Tween 80 AgNPs deposited slower than the other types which means more contact time between the aggregates and heavy metal in surface water.

3.3. Cu, Zn, Pb and Cd dynamics in pore water

The total and colloidal concentrations of Cu in the pore water are shown in Fig. 2. The total concentration of Cu dropped rapidly to 56 ± 1, 39 ± 0.7, 43 ± 1.2, and 42 ± 0.7 μg L^{-1}, respectively after day 1 in the four dosed containers at 1 cm depth, possibly because a big part of AgNPs had settled out from the surface water and entered the pore water of sediment, which would adsorb heavy metals include Cu, causing the metal content to be taken up by the sediment solids. Besides absorption of heavy metals, AgNPs will react with colloidal matters to hetero-aggregates, causing natural colloids that contain heavy metals, to precipitate. It has been reported that humic and fulvic acids can stabilize nanoparticles and ions in the solution (Klaine et al., 2008) because humic acid are likely to form nanoscale coating on solid phases and reduce aggregation by charge stabilization (Bae et al., 2011). In realistic situation, the concentration of natural organic matter is likely to be much higher than the concentration of nanomaterial, so the organic matter would aggregate other than stabilization (Batley et al., 2013). The Smoluchowski coagulation theory indicates that nanoparticles will heteroaggregate rapidly with clays, minerals, and other natural colloids in surface water (Elimelech et al., 1995). This outcome corresponds to the TOC concentration drop at day 1, as AgNPs acted as coagulants, causing heavy metals to be absorbed and deposited into sediment (Ackerman et al., 2015). After day 1, the total concentration of Cu started to increase and reached its peak (97 ± 1.2 μg L^{-1}) at day 8 in Bare AgNPs-dosed container. From day 1 to day 3, concentration of colloidal Cu decreased in other three dosed containers, apart from the Tween 80 AgNPs one. This may be due to the fact that bare AgNPs and citrate AgNPs aggregated and deposited too fast onto the solid phase of the sediment, therefore shortened the contact time of AgNPs and metal ions and colloids in pore water. During this period, the sedimentation of AgNPs from surface water to pore water, the agglomeration of AgNPs and colloids in pore water and the replacement reaction of Ag^+ and other

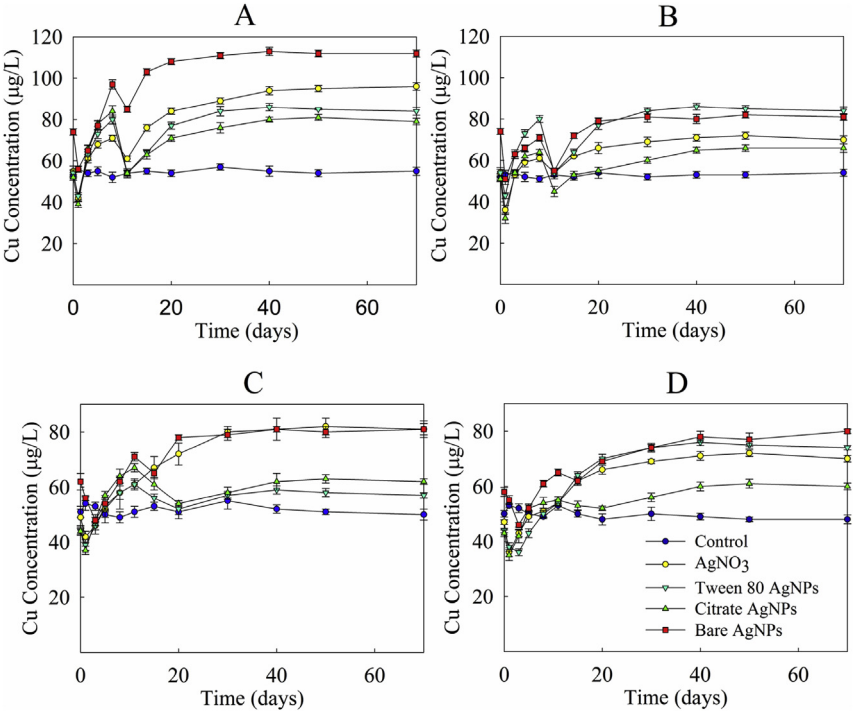

Fig. 2. (A) Changes of total Cu concentration in sediment pore water at 1 cm depth. (B) Concentration of Cu^{2+} in sediment pore water at 1 cm depth. (C) Changes of total Cu concentration in sediment pore water at 3 cm depth. (D) Concentration of Cu^{2+} in sediment pore water at 3 cm depth.

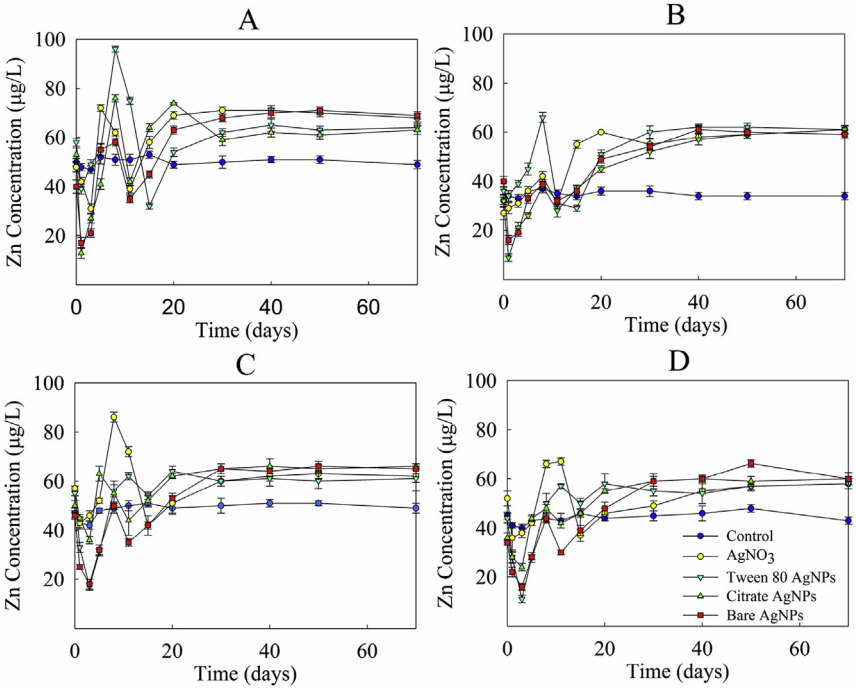

Fig. 3. A) Total concentration of Zn in sediment pore water at 1 cm depth. B) Concentration of Zn^{2+} in pore water at 1 cm depth. C) Total concentration of Zn in sediment pore water at 3 cm depth. D) Concentration of Zn^{2+} in pore water at 3 cm depth.

heavy metals happened simultaneously. The colloidal Cu concentration of all four dosed containers increased mainly due to the decrease of aggregation rate in pore water and the resuspension of particles from sediment surface and the dissolution of Cu^{2+} from sediment between day 3 to day 8. After day 8, AgNPs in surface water had all settled down into solid phase or pore water, the agglomerates of AgNPs in pore water continued to adsorb more heavy metals and deposited into solid phase. The concentration of Cu reached its minimum at day 11, after AgNPs had settled down completely. Then concentration of heavy metals increased, presumably because heavy metals in solid phase started to dissolve and desorption.

The concentration of Zn had the same tendency of Cu as shown in Fig. 3, while concentration of dissolved Pb in 1 cm depth was much lower than in 3 cm depth as shown in Fig. S5. This outcome might be due to the fast diffusion of Pb from sediment to pore water. The fluctuation of Pb and Cd concentration was lower than that of Cu and Zn, because of the lower content in pore water.

Cd concentration decreased after the dose and reached its minimum at day 5 (3 days later than Cu, Zn and Pb) as shown in Fig. S6. Then the concentration of Cd started to increase and reach the equilibrium. Because of the low amount of Cd relative to the added AgNPs, the change of Cd concentration mostly would be due to the adsorption of Cd^{2+} besides particles and colloids contain Cd.

The tendencies of the concentration of four heavy metals in Tween 80 AgNPs-dosed container were displayed in Fig. 4. The concentrations of Cu and Zn are mostly affected, while Cd and Pb are slightly changed. This might be due to a large part of Cu and Zn existed in suspended solid and colloidal form, they were easily affected by the aggregation of AgNPs. Pb and Cd mostly existed in ion form and this caused that they were less affected by AgNPs.

AgNPs, as a new kind of pollutant, have been reported to be toxic to a variety of microorganisms (Jeon et al., 2003; Bosetti et al., 2002) and algae (Lee et al., 2012). Results of the current research demonstrated that apart from the toxicity, AgNPs can affect heavy metals in pore water of sediment. The aggregates of AgNPs and particles contain heavy metals and the adsorption of heavy metal onto aggregates can change the existing form of heavy metals. Compared to the estimated environmental concentration of manufactured AgNPs (0.03–0.08 or 0.04–0.32 μg L^{-1}) (Batley et al., 2013), the initial concentration of 0.1 mg/L was very high, but owing to the special antimicrobial, antiviral, and antifungal properties of AgNPs, the production and application of AgNPs has been increasing rapidly in recent years. Thus, the incidental or accidental release of AgNPs to natural water represents a potential risk.

3.4. Change of Hg concentration and form in pore water

The tendency of Hg concentration is different from Cu, Zn, Pb and Cd as shown in Fig. 5. At day 1, the concentration of Hg changed slightly mainly from dissolved form to colloidal form, because of the AgNPs aggregates in pore water of sediment. At day 5, a large

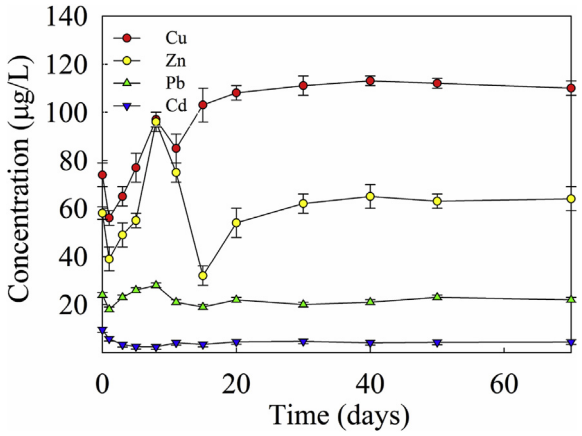

Fig. 4. Total concentration changes of Cu, Zn, Pb and Cd in Tween 80 AgNPs dosed microcosms.

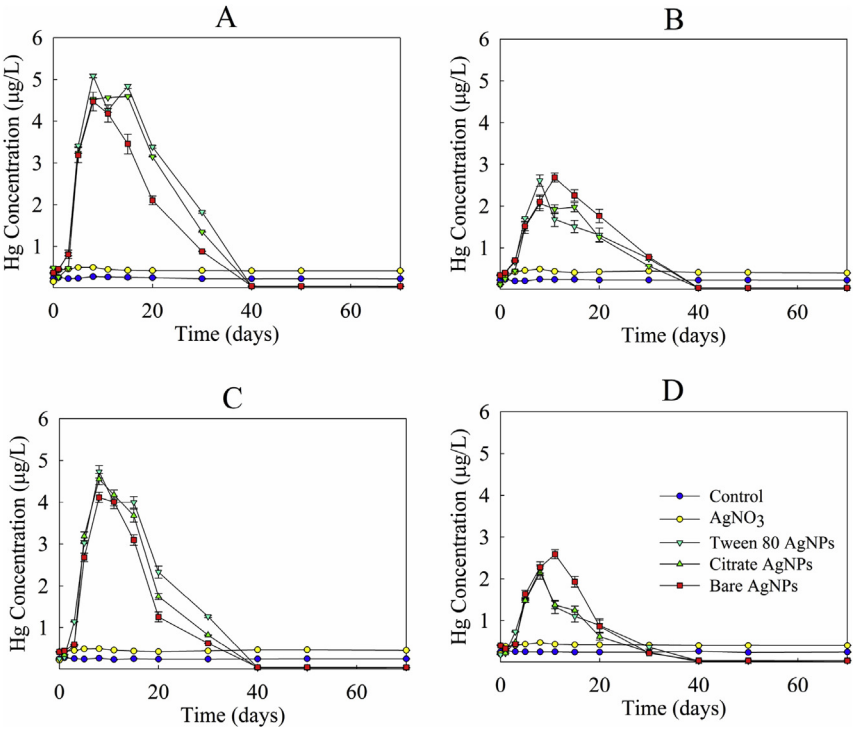

Fig. 5. (A) Total concentration change of Hg in sediment pore water at 1 cm depth. (B) Total concentration change of Hg^{2+} in sediment pore water at 1 cm depth. (C) Total concentration change of Hg in sediment pore water at 3 cm depth. (D) Total concentration change of Hg^{2+} in sediment pore water at 3 cm depth.

increase in Hg concentration was observed, for both the dissolved and the colloidal part. At day 8, the total concentration of Hg in Tween 80 AgNPs dosed container increased to 5.083 ± 0.084 μg L^{-1}, which was also the highest concentration throughout the study. The dissolved aqueous cation of Hg^{2+} makes up a very small portion of total Hg in most environments, including the water column and the aquatic sediments (Skyllberg, 2011; Morel et al., 1998). According to researchers, Hg sorbed onto Fe-minerals can get exchanged, leading to the release of Hg (Jiskra et al., 2014). The increase in the dissolved part was probably because AgNPs caused heavy metal like Cu and Zn to increase, therefore exchanged Hg from colloids and aggregates forming Hg^{2+}, and it will react with S^{2-} to form $HgS_{(s)}$, which may be transformed to $HgS_{(aq)}$ or $HgS(HS)^-$ depending on the solubility constant of $HgS^0_{(aq)}$ (Heileen et al., 2013). As for the colloidal part, Hg^{2+} might have been adsorbed by colloids formed by AgNPs in ionic form or after the formation of HgS. Research from M. S. Bootharaju revealed that Hg^{2+} can be reduced when electrons are supplied by the core atoms of the AgNPs, to form Hg and form a further amalgam with the AgNP core (Bootharaju and Pradeep, 2010).

Ackerman used coagulants to remove mercury from surface water, research showed that due to the transfer of the dissolved Hg into the particulate fraction, particulate total Hg concentration in water in dosed wetlands were higher at the inlets and lower in the outlets compared to the control wetlands (Ackerman et al., 2015). Our research used a still water environment, so the particulate Hg might deposit into the pore water of sediment, and because the AgNPs were added in one dose, along with the adsorption, Hg in sediment might continue to dissolve causing concentration of Hg in pore water of sediment to increase.

3.5. Effect of coating agents and depth

Even though the same tendency of heavy metal concentration of the four dosing containers, different coatings caused the AgNPs to have different characteristics in oxidization, dissolution and agglomeration. Bare AgNPs have the fastest dissolution rate for there was no protection agent to prevent the silver coming into contact with O_2, H^+ and metal ions. In the container dosed with Bare AgNPs, dissolution and aggregation happened significantly rapidly and diminished the adsorption time of heavy metals and aggregates, causing fewer ionic heavy metals to shift to solid form. On the other hand, Tween 80 AgNPs were more stable in water than Bare AgNPs because of the long-chain molecules on the Ag core surface. In the container dosed with Tween 80 AgNPs, AgNPs existed longer than Bare AgNPs in colloidal form in pore water, resulting in a higher metal adsorption. Dissolved heavy metals in the pore water of the container dosed with Tween 80 AgNPs, were lower in concentration than in the ones with citrate AgNPs or Bare AgNPs. In consumer products with AgNPs, AgNPs are required to be stable and the release of Ag + slowly and continuously. However, after released into environment, stable AgNPs might cause more trouble than unstable one which would dissolve or sediment rapidly.

In all containers, the tendency at different depths was similar for most metals, apart from a small delay for Hg. Concentration of Hg in pore water in 3 cm depth increased similarly to that at 1 cm depth (Fig. 5). This may be due to the fast penetration caused by the 100 μgL^{-1} initial concentration of AgNPs. After day 8, Hg concentration started to decrease, and the concentration at 3 cm depth decreased earlier than at 1 cm depth. This may be because some of the colloids at 3 cm depth comes from the colloids at 1 cm depth, these bigger colloids may deposit faster than at 1 cm depth. According to Gregory's report, AgNPs can descend through the sediment to 4 cm depth (Lowry et al., 2012). Also, the concentration of heavy metals at a depth of 3 cm was lower than at 1 cm depth because of the delay. According to previous research, dosed AgNPs was primarily present in the upper layer of the surface sediment

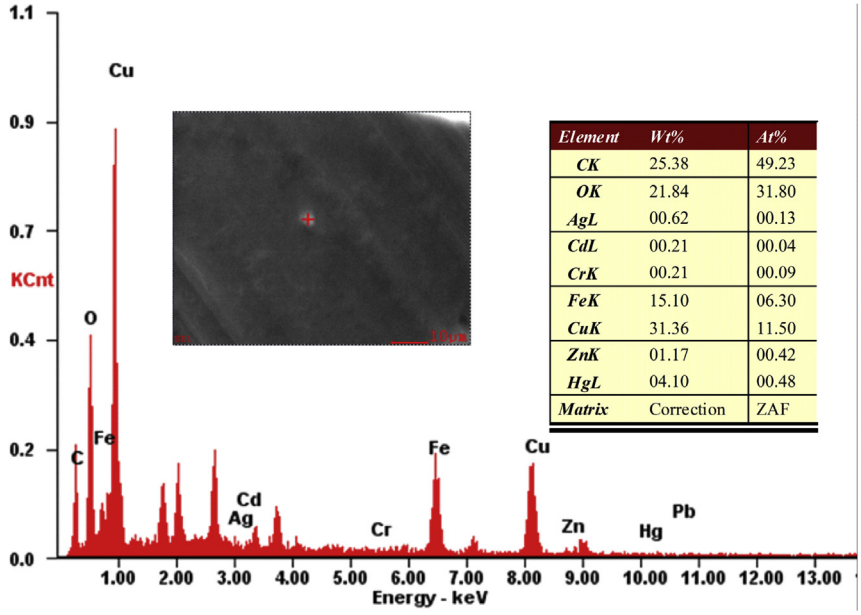

Fig. 6. SEM images and EDX analysis of pore water particles.

(0–1 cm) (Lowry et al., 2012) which suggests that the change of heavy metal concentration and form in this research only occurred in the upper layer of sediment. This raises the concern that the aggregates with large Hg content would transport with the flow in a natural river.

3.6. SEM-EDX analysis

To gain further insight into the components of colloids in sediment pore water, dry colloids were analyzed by SEM and EDX. As shown in Fig. 6, SEM images revealed that the size of the particles was increased to several μm possibly because of the drying process. EDX analysis showed that particles in pore water had a low content of Zn, Pb and Cd (because of the background of the Cu grid, Cu had very high peak in EDX analysis). This can be explained by the fact that most heavy metals existed in dissolved form after day 8. Even though the concentration of Hg was high, Hg was not detected in most parts of colloids in pore water. Hg was mostly detected in those colloids that contained Ag. Surprisingly, the Hg content showed a good linear correlation with the Ag content as shown in Fig. 7. The Hg/Ag ratio was approximately 4. It is very possible that Hg had formed an amalgam with AgNPs. Research reports that Hg(II) can be reduced to Hg(0) and be incorporated into the metallic Cu, while the association of Ag with metallic Cu nanoparticles is also noticed (Hofacker et al., 2013). In this study, different from the Cu nanoparticles, the AgNPs were added artificially, so it is unlikely that Hg(II) was incorporated into the aggregates. On the other hand, Hg(II) might have been reduced to Hg(0) and formed an amalgam with AgNPs, causing colloidal Hg concentration to increase. Unfortunately, due to the low sample content, we failed to collect enough pore water colloids to analyze the valence of Hg elements.

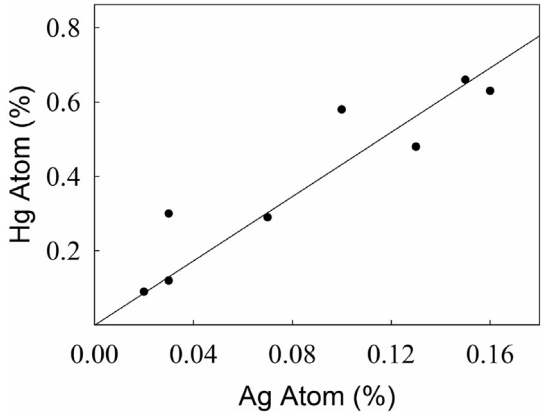

Fig. 7. Correlation fit of Ag atoms content and Hg atoms content in sediment pore water colloids.

4. Conclusions

This research was conducted with sediment and surface water contaminated with heavy metals from the Xiangjiang River. The results showed that in addition to current metal pollution status, AgNPs may act as a coagulant that can deposit ions and colloids containing Cu, Zn, Pb, and Cd from pore water of sediment, causing decrease in heavy metal concentration. On the other hand, part of AgNPs might stabilize in pore water and form an Ag-Hg amalgam, which may represent an important kind of Hg transformation in the sediment. This study has shown that Hg-Ag amalgam formation can cause substantial colloidal Hg mobilization to surface water and be transported through the stream to unpolluted areas. Thus the Hg-Ag amalgam nanoparticles may significantly contribute to Hg transport across large distances, upon their release into surface water. Further studies should be conducted to investigate the transport of colloids in sediment pore water, which contains heavy metal induced by AgNPs, from polluted source points to unpolluted areas.

Acknowledgment

This study was financially supported by the National Natural Science Foundation of China (51579099 and 51521006), the Program for Changjiang Scholars and Innovative Research Team in University (IRT-13R17), the Hunan Provincial innovation Foundation For Postgraduate (CX2016B134).

Appendix A. Supplementary data

Supplementary data related to this article can be found at http://dx.doi.org/10.1016/j.chemosphere.2016.07.043.

References

Ackerman, J.T., Kraus, T.E.C., Fleck, J.A., 2015. Experimental dosing of wetlands with coagulants removes mercury from surface water and decreases mercury bioaccumulation in fish. Environ. Sci. Technol. 49, 6304–6311.

Bae, E., Park, H.J., Yoon, J., et al., 2011. Bacterial uptake of silver nanoparticles in the presence of humic acid and $AgNO_3$. Korean J. Chem. Eng. 28, 267–271.

Batley, G.E., Kirby, J.K., Mclaughlin, M.J., 2013. Fate and risks of nanomaterials in aquatic and terrestrial environments. Acc. Chem. Res. 46, 854–862.

Benn, T.M., Westerhoff, P., 2008. Nanoparticles silver released into water from commercially available sock fabrics. Environ. Sci. Technol. 42, 4133–4139.

Bielmyer, G.K., Bell, R.A., Klain, S.J., 2002. Effects of ligand-bound silver on *Ceriodaphnia dubia*. Environ. Toxicol. Chem. 21, 2204–2208.

Blaser, S.A., Scheringer, M., MacLeod, M., 2008. Estimation of cumulative aquatic exposure and risk due to silver: contribution of nano-functionalized plastics and textiles. Sci. Total Environ. 390, 396–409.

Bootharaju, M.S., Pradeep, T., 2010. Uptake of toxic metal ions from water by naked and monolayer protected silver nanoparticles: an X-ray photoelectron spectroscopic investigation. J. Phys. Chem. *C* 114, 8328–8336.

Bosetti, M., Masse, A., Tobin, E., 2002. Silver coated materials for external fixation devices: in vitro biocompatibility and genotoxicity. Biomaterials 23, 887–892.

Boxall, A.B.A., Chaudhry, Q., Sinclair, C., 2007. Current and Future Predicted Environmental Exposure to Engineered Nanoparticles. Department of Environment Food and Rural Affairs.

Chambers, B.A., Nabiul Afrooz, A.R.M., Bae, Sungwoo, 2014. Effects of chloride and ionic strength on physical morphology, dissolution, and bacterial toxicity of silver nanoparticles. Environ. Sci. Technol. 48, 761–769.

Edmondson, J.L., Scott, I., Potter, J., et al., 2015. Black carbon contribution to organic carbon stock in urban soil. Environ. Sci. Technol. 49, 8339–8346.

Elimelech, M., Jia, X., Gregory, J., 1995. Particle Deposition and Aggregation: Measurement, Modelling and Simulation. Butterworth-Heinemann, Boston, p. 448.

Guo, Z., Chen, G.Q., Liu, L.Z., et al., 2016. Activity variation of Phanerochaete chrysosporium under nanosilver exposure by controlling of different sulfide sources. Sci. Rep. 6, 20813–20818.

He, D., Dorantes-Aranda, J.J., Waite, T.D., 2012. Silver nanoparticle-Algae interactions: oxidative dissolution, reactive oxygen species generation and synergistic toxic effects. Environ. Sci. Technol. 46, 8731–8738.

Heileen, H.K., Kucharzyk, K.H., Zhang, Tong, 2013. Mechanisms regulating mercury bioavailability for methylating microorganisms in the aquatic environment: a critical review. Environ. Sci. Technol. 47, 2441–2456.

Hofacker, A.F., Voegelin, A., Kaegi, R., 2013. Mercury mobilization in a flooded soil by incorporation into metallic copper and metal sulfide nanoparticles. Environ. Sci. Technol. 47, 7739–7746.

Jeon, H.J., Yi, S.C., Oh, S.G., 2003. Preparation and antibacterial effects of Ag-SiO_2 thin films by Sol-Gel method. Biomaterials 24, 4921–4928.

Jiskra, M., Saile, D., Wiederhold, J.G., 2014. Kinetics of Hg(II) exchange between organic ligands, goethite, and natural organic matter studied with an enriched stable isotope approach. Environ. Sci. Technol. 48, 13207–13217.

Jones, C.M., Hoek, Eric M.V., 2010. A review of the antibacterial effects of silver nanomaterials and potential implications for human health and the environment. J. Nanopart. Res. 12, 1531–1551.

Klaine, S.J., Alvarez, P.J.J., Batley, G.E., et al., 2008. Nanomaterials in the environment: behavior, fate, bioavailability, and effects. Environ. Toxicol. Chem. 9, 1825–1851.

Kvitek, L., Panacek, A., Soukupova, J., 2008. Effect of surfactants and polymers on stability and antibacterial activity of silver nanoparticles (NPs). J. Phys. Chem. C 112, 5825–5834.

Lee, W.M., Kwak, J.I., An, Y.J., 2012. Effect of silver nanoparticles in crop plants *phaseolus radiatus* and *sorghum bicolor*: media effect on phytotoxicity. Chemosphere 86, 491.

Li, X., Lenhart, J.J., 2012. Aggregation and dissolution of silver nanoparticles in natural surface water. Environ. Sci. Technol. 46, 5378–5386.

Li, L.X.Y., Hartmann, G., Döblinger, M., Schuster, M., 2013. Quantification of nanoscale silver particles removal and release from municipal wastewater treatment plants in Germany. Environ. Sci. Technol. 47, 7317–7323.

Lin, D.H., Tian, X.L., Wu, F.C., 2010. Fate and transport of engineered nanomaterials in the environment. J. Environ. 39, 1896–1908.

Lowry, G.V., Espinasse, B.P., Badireddy, A.R., 2012. Long-term transformation and fate of manufactured Ag nanoparticles in a simulated large scale freshwater emergent wetland. Environ. Sci. Technol. 46, 7027–7036.

Mao, L.J., Mo, D.W., Yang, J.H., 2014. Rare earth elements geochemistry in surface floodplain sediments from the Xiangjiang River, middle reach of Changjiang River, China. Quat. Int. 336, 80–88.

Morel, F.M.M., Kraepiel, A.M.L., Amyot, M., 1998. The chemical cycle and bioaccumulation of mercury. Annu. Rev. Ecol. Syst. 29, 543–566.

Mueller, N.C., Nowack, Bernd, 2008. Exposure modeling of engineered nanoparticles in the environment. Environ. Sci. Technol. 42, 4447–4453.

Piccapietra, F., Sigg, L., Behra, R., 2012. Colloidal stability of carbonate-coated silver nanoparticles in synthetic and natural freshwater. Environ. Sci. Technol. 46, 818–825.

Rawlins, B.G., Vane1, C.H., Kim, A.W., et al., 2008. Methods for estimating types of soil organic carbon and their application to surveys of UK urban areas. Soil Use Manag. 24, 47–59.

Shoults-Wilson, W.A., Reinsch, B.C., Tsyusko, O.V., 2013. Role of particle size and soil type in toxicity of silver nanoparticles to earthworms. Soil Sci. Soc. Am. J. 75, 365–377.

Skyllberg, U., 2011. Chemical Speciation of mercury in soil and sediment. Cheminform 44, 219–258.

Unrine, J.M., Colman, B.P., Bone, A.J., 2012. Biotic and abiotic interactions in aquatic microcosms determine fate and toxicity of Ag nanoparticles: Part 1-aggregation and dissolution. Environ. Sci. Technol. 46, 6915–6924.

Unrine, J.M., Colman, B.P., Bone, A.J., 2012. Biotic and abiotic interactions in aquatic microcosms determine fate and toxicity of Ag nanoparticles: Part 2- Toxicity and Ag speciation. Environ. Sci. Technol. 46, 6925–6933.

Vignati, D., Dominik, J., 2003. The role of coarse colloids as a carrier phase for trace metals in riverine systems. Aquat. Sci. 65, 129–142.

Zhu, H.N., Yuan, X.Z., Zeng, G.G., 2012. Ecological risk assessment of heavy metals in sediments of Xiawan Port based on modified potential ecological risk index. Trans. Nonferr. Met. SOC. China 22, 1470–1477.

Zuo, Y.N., Chen, G.Q., Zeng, G.M., et al., 2015. Transport, fate, and stimulating impact of silver nanoparticles on the removal of Cd(II) by *Phanerochaete chrysosporium* in aqueous solutions. J. Hazard. Mater. 285, 236–244.